Cytoplasmic linker proteins promote microtubule rescue in vivo

Yulia A. Komarova,[1] Anna S. Akhmanova,[2] Shin-ichiro Kojima,[1] Niels Galjart,[2] and Gary G. Borisy[1]

[1]Department of Cell and Molecular Biology, Northwestern University Medical School, Chicago, IL 60611
[2]Department of Cell Biology and Genetics, Erasmus University, 3015 GE Rotterdam, Netherlands

The role of plus end–tracking proteins in regulating microtubule (MT) dynamics was investigated by expressing a dominant negative mutant that removed endogenous cytoplasmic linker proteins (CLIPs) from MT plus ends. In control CHO cells, MTs exhibited asymmetric behavior: MTs persistently grew toward the plasma membrane and displayed frequent fluctuations of length near the cell periphery. In the absence of CLIPs, the microtubule rescue frequency was reduced by sevenfold. MT behavior became symmetrical, consisting of persistent growth and persistent shortening. Removal of CLIPs also caused loss of p150^{Glued} but not CLIP-associating protein (CLASP2) or EB1. This result raised the possibility that the change in dynamics was a result of the loss of either CLIPs or p150^{Glued}. To distinguish between these possibilities, we performed rescue experiments. Normal MT dynamics were restored by expression of the CLIP-170 head domain, but p150^{Glued} was not recruited back to MT plus ends. Expression of p150^{Glued} head domain only partially restored MT dynamics. We conclude that the CLIP head domain is sufficient to alter MT dynamics either by itself serving as a rescue factor or indirectly by recruiting a rescue factor. By promoting a high rescue frequency, CLIPs provide a mechanism by which MT plus ends may be concentrated near the cell margin.

Introduction

The dynamic behavior of microtubules (MTs)* is essential for the cytoskeletal remodeling underlying the fundamental processes of cell morphogenesis, cell motility, and cell division. Consequently, MT dynamics are likely to be highly regulated, and numerous proteins including MT-associated proteins (MAPs) and molecular motors have been proposed as possible regulatory factors (Heald, 2000; Hunter and Wordeman, 2000; Tournebize et al., 2000; Spittle et al., 2000; Kinoshita et al., 2001; Vorobjev et al., 2001). MTs have an intrinsic structural polarity and are generally oriented in cells with their minus ends at the centrosome and their plus ends pointing toward the cell periphery. Their dynamics consist of alternating phases of growth and shortening, a pattern of behavior known as dynamic instability (Mitchison and Kirschner, 1984). Recently, a group of proteins that specifically bind to the MT plus end has been identified (Perez et al., 1999;

Vaughan et al., 1999; Hoogenraad et al., 2000; Mimori-Kiyosue et al., 2000a,b; Akhmanova et al., 2001; Coquelle et al., 2002). These proteins are particularly attractive candidates as regulatory factors.

Cytoplasmic linker protein (CLIP)-170 is the founding member of the MT plus end family and was originally identified as a protein essential for binding of endocytic vesicles to MTs (Rickard and Kreis, 1990; Pierre et al., 1992). Subsequently, it was shown that CLIP-170 has the unusual property of binding specifically to the ends of growing, not stable or shortening MTs (Perez et al., 1999). Its strategic location at the ends of growing MTs is consistent with a role in regulation of MT dynamics in addition to possible roles in organelle or cortical targeting.

Recently, we reinvestigated MT dynamics in animal cells containing a centrosomally based pattern of MTs (Komarova et al., 2002). We found that MT behavior deep in the cell interior differed from that at the cell periphery (Sammak et al., 1987; Cassimeris et al., 1988; Shelden and Wadsworth, 1993; Waterman-Storer and Salmon, 1997; Yvon and Wadsworth, 1997), where for technical reasons most previous observations had been made. We found that nascent MTs grew persistently from the centrosome to the cell margin. Only near the cell margin did MTs alternate between the phases of shortening and growth characteristic of dynamic instability. In contrast to growth, shortening of MTs back

from the cell margin was not persistent. A question posed by these results was whether the persistent growth was the result of a plus end factor or was the constitutive behavior of MTs.

Genetic analysis in the fission yeast, *Schizosaccharomyces pombe*, identified Tip1, an ortholog of CLIP-170, which was shown to be involved in guidance of MTs to the cell ends (Brunner and Nurse, 2000). Tip1p was proposed to be a suppressor of MT catastrophe that distinguished between the general cell cortex and the cell ends. The persistent growth of MTs we observed in mammalian cells suggested that CLIP-170 might serve a role similar to that of tip1p in fission yeast.

To evaluate this possibility, it was necessary to remove endogenous CLIPs from the plus ends of MTs in vivo and to determine quantitatively the consequences on MT dynamics. In its simplest form, MT dynamics are characterized by four parameters, the velocities of growth and shortening and the transition frequencies, catastrophe and rescue, between the growth and shortening phases. We determined these parameters and found that persistent MT growth did not depend on the presence of CLIPs, indicating that in mammalian cells it did not function as an anticatastrophe factor. In contrast, removal of CLIPs reduced the rescue frequency resulting in long excursions of shortening. We conclude that in addition to possible roles in organelle or membrane targeting CLIPs function either directly or indirectly as rescue factors in MT dynamics.

Results

CLIP-170 Δhead expression removes endogenous CLIPs from MT plus ends

We sought to devise a dominant negative mutant that could be used to investigate the function of CLIPs in regulating MT dynamics in vivo. CLIP-170 and CLIP-115 are two paralogs of the CLIP family in mammals (Hoogenraad et al., 2000). Both proteins contain two conserved MT-binding CAP-Gly motifs (MTB) at the NH$_2$ terminus (termed the head) followed by a long stretch of heptad α-helical repeats responsible for homodimer formation, presumably by a coiled-coil mechanism (Perez et al., 1999; Scheel et al., 1999; Hoogenraad et al., 2000). The COOH terminus of CLIP-170 has two metal-binding motifs which are absent in CLIP-115. Based on this structure, we surmised that a construct lacking the head (MT-binding domain) might serve as a dominant negative mutant for both CLIP species.

As shown previously, GFP fusions of CLIP-170 or CLIP-170 head domain bind to MT plus ends in vivo (Diamantopoulos et al., 1999; Perez et al., 1999), whereas deletion of the head domain abolished the capacity of the polypeptide to bind to MTs (Pierre et al., 1994). Therefore, we made an EGFP fusion of a CLIP-170 Δhead construct and an EGFP fusion of the head alone that served as a control (Fig. 1 A). The effects of the constructs were analyzed by transient expression in CHO-K1 and COS-7 cells. Confirming previous results (Diamantopoulos et al., 1999; Perez et al., 1999), full-length EGFP–CLIP-170 tracked MT plus ends (unpublished data). Although COS-7 cells contain only CLIP-170, CHO-K1 cells contain both CLIP-170 and CLIP-115. Therefore, to determine the distribution of endogenous

CLIPs we used an antibody (#2221; see Materials and methods) that recognized both species (Hoogenraad et al., 2000). Overexpression of the EGFP–CLIP-170 Δhead mutant caused a reduction in the level of endogenous CLIP staining at MT plus ends and an elevation of CLIP staining distributed through the cytoplasm, whereas neighboring untransfected cells showed normal plus end staining (Fig. 1 B). Similar results were obtained in COS-7 cells (unpublished data). The level of CLIPs remaining at MT plus ends was quantified by measuring the fluorescent signal in the CLIP channel relative to the signal in the tubulin channel within a square box 5 pixels (0.45 μm) on a side (see Materials and methods). Expression of the CLIP-170 Δhead mutant reduced the CLIP signal to 7.2 ± 1.4% (SEM) compared with control cells (n = 76 MT plus ends for experimental cells; 86 plus ends for control cells). Therefore, we conclude that overexpression of the CLIP-170 Δhead mutant removed almost all of both CLIP paralogs from MT plus ends.

Immunoprecipitation (IP) analysis was performed to identify whether the CLIP-170 Δhead mutant removed endogenous CLIPs by interacting with them. Fig. 1 C (left) shows that EGFP fusions were expressed as single protein species of appropriate molecular weight in cell extracts, which could be immunoprecipitated with an antibody to GFP and that no degradation products were evident. Fig. 1 C (right) shows a similar experiment probed with antibody to the CLIP head (no. 2221). The antibody gave the expected strong reaction in cell extracts with expressed full-length EGFP–CLIP-170 and expressed CLIP-170 head and with endogenous CLIP-170 and CLIP-115, whereas expressed CLIP-170 Δhead gave a weak cross-reaction (Fig. 1 C, asterisk). In addition, the antibody reacted with an unknown species of 90 kD. The IP lanes revealed no interaction between endogenous CLIPs and overexpressed full-length EGFP–CLIP-170 or EGFP–CLIP-170 head but did reveal an interaction of CLIP-115 with the EGFP–CLIP-170 Δhead mutant (ΔH). Note that in Fig. 1 C, the top band in the ΔH IP lane corresponds to a cross-reaction with the EGFP–CLIP-170 Δhead protein and not to endogenous CLIP-170. To evaluate whether the EGFP tag interfered with an interaction between the Δhead mutant and CLIP-170 (but not CLIP-115), the IP experiments were repeated, substituting an HA tag for EGFP. HA-tagged CLIP-170Δ head protein was expressed and pulled down with antibody to the HA epitope, and the blots were probed antibody to the CLIP head as before. The HA–CLIP-170 Δhead mutant migrated differently from its EGFP chimera, allowing it to be more clearly distinguished from endogenous CLIP-170. Again, the IP pulled down endogenous CLIP-115 but not CLIP-170 (unpublished data). The direct interaction of the CLIP-170 Δhead mutant with CLIP-115 suggests a simple binding and sequestering mechanism for loss of endogenous CLIP-115 from MT plus ends. However, the lack of a direct interaction of the CLIP-170 Δhead mutant with endogenous CLIP-170 suggests that a different mechanism is necessary to explain removal of CLIP-170. Possibly, the difference in response is related to the COOH-terminal metal-binding motif present in CLIP-170 but absent in CLIP-115 (see Discussion). Nevertheless, the significant point for this study is that the CLIP-170 Δhead mutant removed both
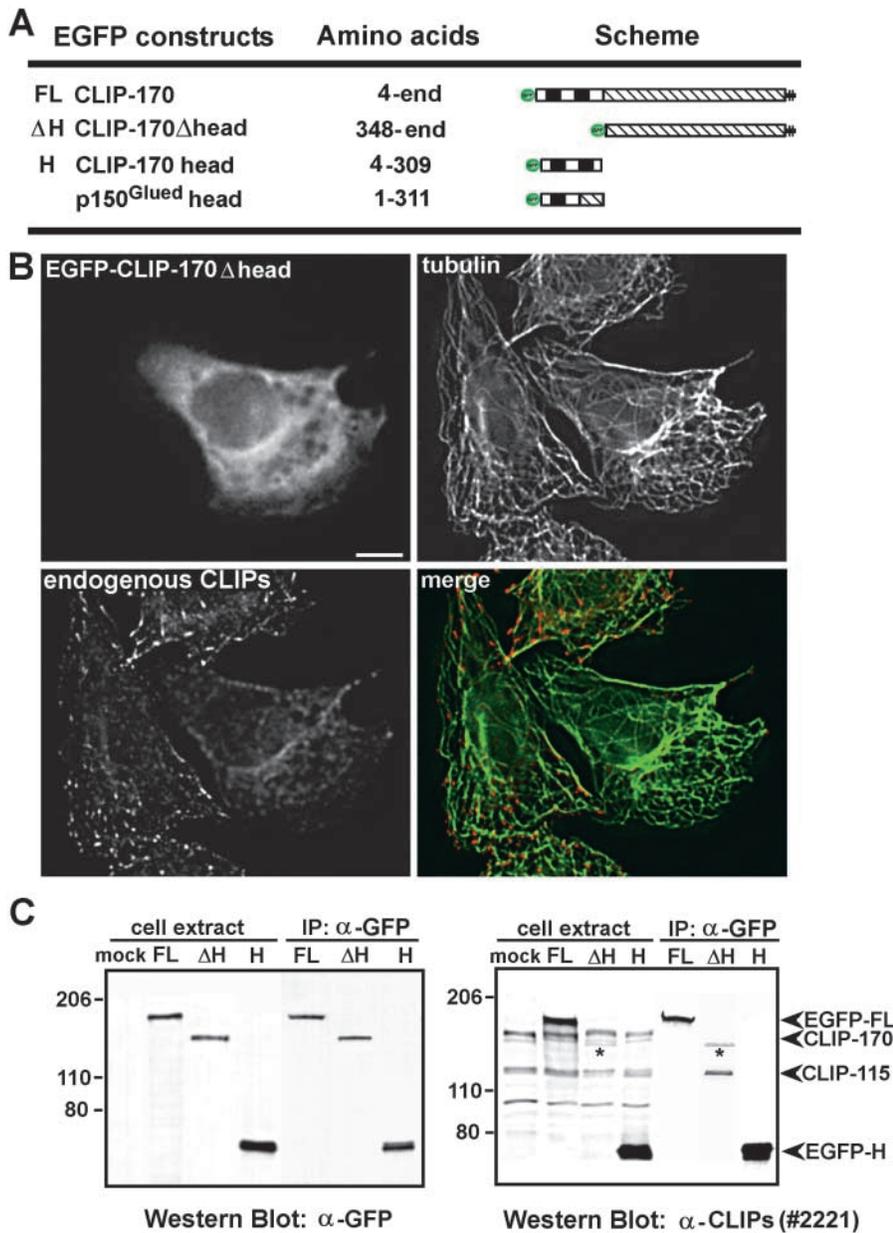
A

EGFP constructs — **Amino acids** — **Scheme**

EGFP constructs	Amino acids
FL CLIP-170	4-end
ΔH CLIP-170Δhead	348-end
H CLIP-170 head	4-309
p150^{Glued} head	1-311

B EGFP-CLIP-170Δhead / tubulin / endogenous CLIPs / merge

C cell extract — IP: α-GFP / cell extract — IP: α-GFP

Western Blot: α-GFP

Western Blot: α-CLIPs (#2221)

◄EGFP-FL
◄CLIP-170
◄CLIP-115
◄EGFP-H

Figure 1. **CLIP-170 Δhead serves as a dominant negative mutant.** (A) Schematic representation of EGFP fusion constructs of CLIP-170 and p150^{Glued}. Black bars represent MT-binding domains, hatched bar represents coiled-coil region, COOH-terminal antenna-like structure represents metal-binding motifs. FL denotes full-length EGFP–CLIP-170, Δhead EGFP–CLIP-170 deletion of head domain (CLIP-170 ΔH), and H denotes EGFP–CLIP-170 head. (B) Distribution of endogenous CLIPs in CHO-K1 control cells and cell expressing EGFP–CLIP-170 Δhead mutant. Polyclonal antibody (no. 2221; as described in Materials and methods) recognizing the head domain of both CLIP-170 and CLIP-115 was used to visualize CLIP distribution. Immuno-staining showed no CLIPs at MT plus ends in the EGFP-positive cell, whereas a strong signal was evident in control cells. (Merged image) Green is tubulin and red is CLIP. Bar, 10 μm. (C) Western blotting and IP analysis. CHO-K1 cells were mock transfected or transfected with EGFP fusion constructs of CLIP-170 (FL), CLIP-170 Δhead (ΔH), or CLIP-170 head (H), and analyzed directly or immunoprecipitated with anti-GFP antibody. (Left) Samples were probed with GFP antibody. Cell extract lanes (mock, FL, ΔH, and H) showed that mock transfection gave a clean background; single bands in the other lanes showed that expressed constructs produced soluble proteins of predicted size of ∼190, 150, and 65 kD for full-length EGFP–CLIP-170, EGFP–CLIP-170 ΔH, and EGFP–CLIP-170 head, respectively. IP lanes (FL, ΔH, and H) showed that proteins were efficiently immunoprecipitated by GFP antibody. (Right) Samples were probed with anti-CLIP head antibody. Cell extract lanes (mock, FL, ΔH, and H) show reaction of head antibody with endogenous and expressed CLIP-170 proteins. IP lanes (FL, ΔH, and H) show that CLIP-115 is immunoprecipitated along with the EGFP–CLIP-170 Δhead but not with EGFP–CLIP-170 full-length or EGFP–CLIP-170 head mutant. Endogenous CLIP-170 showed no interaction with any construct.

CLIP species from MT plus ends and served as a dominant negative mutant.

Absence of CLIPs at MT plus ends abolishes MT rescue

MT dynamics in nontransfected CHO-K1 cells (Komarova et al., 2002) or in control CHO-K1 cells expressing the EGFP vector (Table I) were indistinguishable as assayed by determining the four basic parameters of dynamic instability: the rates of MT growth and shortening and the transition frequencies from shortening phase to growth phase (rescue) and growth phase to shortening phase (catastrophe). A principal feature of the MT life cycle was the asymmetric character of the growth and shortening phases. Growth in the cell interior was persistent with arrival of plus ends at the cell margin frequently occurring without a catastrophe

(k_{cat} = 0.003 s^{-1}). In contrast, near the cell margin episodes of shortening alternated with episodes of growth (k_{res} = 0.17 s^{-1}), leading to a fluctuation type behavior (Fig. 2, A and B). The length of shortening episodes was distributed exponentially (mean = 3.7 ± 2.8 μm) (Fig. 2 C) reflective of a stochastic process. The high rescue frequency resulted in concentration of the plus ends at the cell periphery as demonstrating by an ascending distribution of MT length from the centrosome toward the cell edge (Fig. 2 D).

Absence of CLIPs at the growing plus ends, induced by overexpression of the CLIP-170 Δhead mutant, caused a profound change in the pattern of MT dynamics; namely, MT behavior became symmetric. Growth and shortening velocities were not affected (Table I). The catastrophe frequency was also not affected. MTs grew persistently from the cen-

Table I. **MT dynamics parameters quantified upon expression of different constructs**

	Growth rate, v_g[a]	Shortening rate, v_s[a]	Catastrophe frequency, k_{cat}[b]	Rescue frequency, k_{res}[b]
	$\mu m\ min^{-1}$	$\mu m\ min^{-1}$	s^{-1}	s^{-1}
Control:	21.5 ± 8.2	35.6 ± 12.8	0.003 ± 0.002	0.17 ± 0.03
EGFP	65 MTs	403 MTs	65 MTs	403 MTs
Dominant negative:	21.8 ± 13.0	33.7 ± 19.0	0.005 ± 0.006	0.024 ± 0.005
EGFP–CLIP-170 Δhead	76 MTs	76 MTs	76 MTs	400 MTs
Rescue experiment I:	19.6 ± 11.7	33.6 ± 13.6	0.003 ± 0.002	0.16 ± 0.03
EBFP–CLIP-170 Δhead + EGFP–CLIP-170 head	91 MTs	400 MTs	91 MTs	400 MTs
Rescue experiment II:	19.0 ± 6.9	30.0 ± 9.4	0.004 ± 0.003	0.05 ± 0.016
EBFP–CLIP-170 Δhead + EGFP-p150[Glued] head	71 MTs	350 MTs	71 MTs	350 MTs

[a]Growth and shortening rates and SDs were calculated from frequency histograms of instantaneous rates.
[b]Catastrophe and rescue frequencies were calculated from MT life histories for each cell as the number of transition events over integrated time of observation of individual phases; numbers given are average and SD for the population of cells. Number of transition events and integrated times were as follows: control, 12 catastrophes for 2,337 s and 385 rescues for 2,248 s; dominant negative, 9 catastrophes for 1,328 s and 141 rescues for 6,096 s; rescue experiment I, 8 catastrophes for 2,604 s and 397 rescues for 2,556 s; rescue experiment II, 11 catastrophes for 3,156 s and 254 rescues for 5,558 s.

trosome toward the cell margin as in control cells. The striking difference was that shortening MTs were not rescued at high frequency. Most MTs (65%) that arrived at the cell margin shortened persistently all the way back to the centrosome (Fig. 2, E and F). Analysis of life history plots indicated that the rescue frequency was reduced sevenfold with the consequence that the average length of shortening excursions became greatly increased (10.9 ± 4.0 μm) and in many instances was limited only by the distance to the centrosome (Fig. 2 G). The low rescue frequency of MT dynamics led to an equal distribution of MT plus ends throughout the cytoplasm (Fig. 2 H). The failure of MTs to be rescued decreased dramatically the average lifetime of a MT. MT lifetimes, estimated for control cells as ∼20 min, became less then 1 min in the absence of CLIPs (46 ± 32 s, $n = 25$). Comparable results were obtained for MT dynamics in COS-7, NRK, and BHK-21 cells expressing the EGFP–CLIP-170 Δhead mutant (unpublished data). Thus, the effect of removing CLIPs from the plus ends of MTs seems to be general. The results suggest that CLIPs serve as rescue factors in regulation of MT behavior and that they are responsible for the accumulation of dynamic plus ends at the cell periphery.

Dependence of other plus end–tracking proteins on removal of CLIPs

The alteration of MT dynamics upon removing CLIPs from MT plus ends suggested that CLIPs are necessary for asymmetric MT behavior. However, since other proteins are also known to track MT plus ends it was possible that regulation of MT dynamics might involve an interaction between CLIP and one or more of these other factors. Evidence has been presented that dynein/dynactin is targeted to MT plus ends by CLIP-170 (Valetti et al., 1999) with a CLIP-170–LIS1 interaction playing a key role in dynactin recruitment (Coquelle et al., 2002; Tai et al., 2002). CLIP-115 and -170–associating proteins (CLASPs) are proteins that associate with both CLIPs and have been suggested to be involved in regulation of MT dynamics (Akhmanova et al., 2001). EB1 is a plus end–tracking protein thought to be targeted to MT plus ends independently of CLIPs (K. Vaughan, personal communication).

We tested whether the localization at MT plus ends of p150[Glued] (a component of dynactin), CLASP2, and EB-1

depended upon the presence of CLIPs. The EGFP–CLIP-170 Δhead mutant was expressed in CHO-K1 or COS-7 cells that were then processed by immunostaining for tubulin and the plus end proteins. Endogenous p150[Glued] was depleted from MT plus ends in transfected but not control cells (Fig. 3 A). Fluorescence quantification showed a reduction in the p150[Glued] signal to $13.4 \pm 1.2\%$ of untransfected cells (101 MT plus ends experimental; 113 control). In contrast, both endogenous CLASP2 and EB1 were still present on MT plus ends at levels similar to that of untransfected cells (Fig. 3, B and C). Quantification of the CLASP2 and EB1 signals gave $94.4 \pm 5.1\%$ and $94.3 \pm 7.1\%$, respectively compared with control level ($n = 134$ and 132 MT plus ends for experimental and control cells for CLASP; 97 and 88, respectively, for EB1). IP experiments showed interaction of the EGFP–CLIP-170 Δhead mutant with p150[Glued] and CLASP2 but not with EB1 (Fig. 3 D). The EGFP–CLIP-170 head showed no interaction with p150[Glued] or CLASP2, confirming that the interaction was mediated solely through the CLIP-170 tail domain. These IP results agree with published data reflecting the interaction of CLIP-170 with p150[Glued] and CLASP2 (Akhmanova et al., 2001; Coquelle et al., 2002). The presence of CLASP2 on MT plus ends in cells expressing the CLIP-170 Δhead mutant suggests that CLASP2, in addition to interacting with the CLIP coil-coil domain, is independently targeted to MTs. This result is consistent with the localization at MT plus ends of CLASP mutants defective in their CLIP binding domain (Akhmanova et al., 2001). Since CLASP2 and EB1 remained on MT plus ends after removal of endogenous CLIPs, it seems unlikely that either of these proteins is directly involved in the observed changes in MT dynamics. On the other hand, the removal of p150[Glued] raises the possibility that the dynein–dynactin complex contributes to CLIP function.

CLIP-170 head domain is sufficient to promote MT rescue

Previous experiments showed that the head domain of CLIP-170 (aa 1–350; termed H1) was monomeric, localized to MT plus ends, and bound to tubulin oligomers with high affinity (Diamantopoulos et al., 1999; Scheel et al., 1999). Based on these results, we thought that the CLIP head might be sufficient to restore normal MT dynamics. To
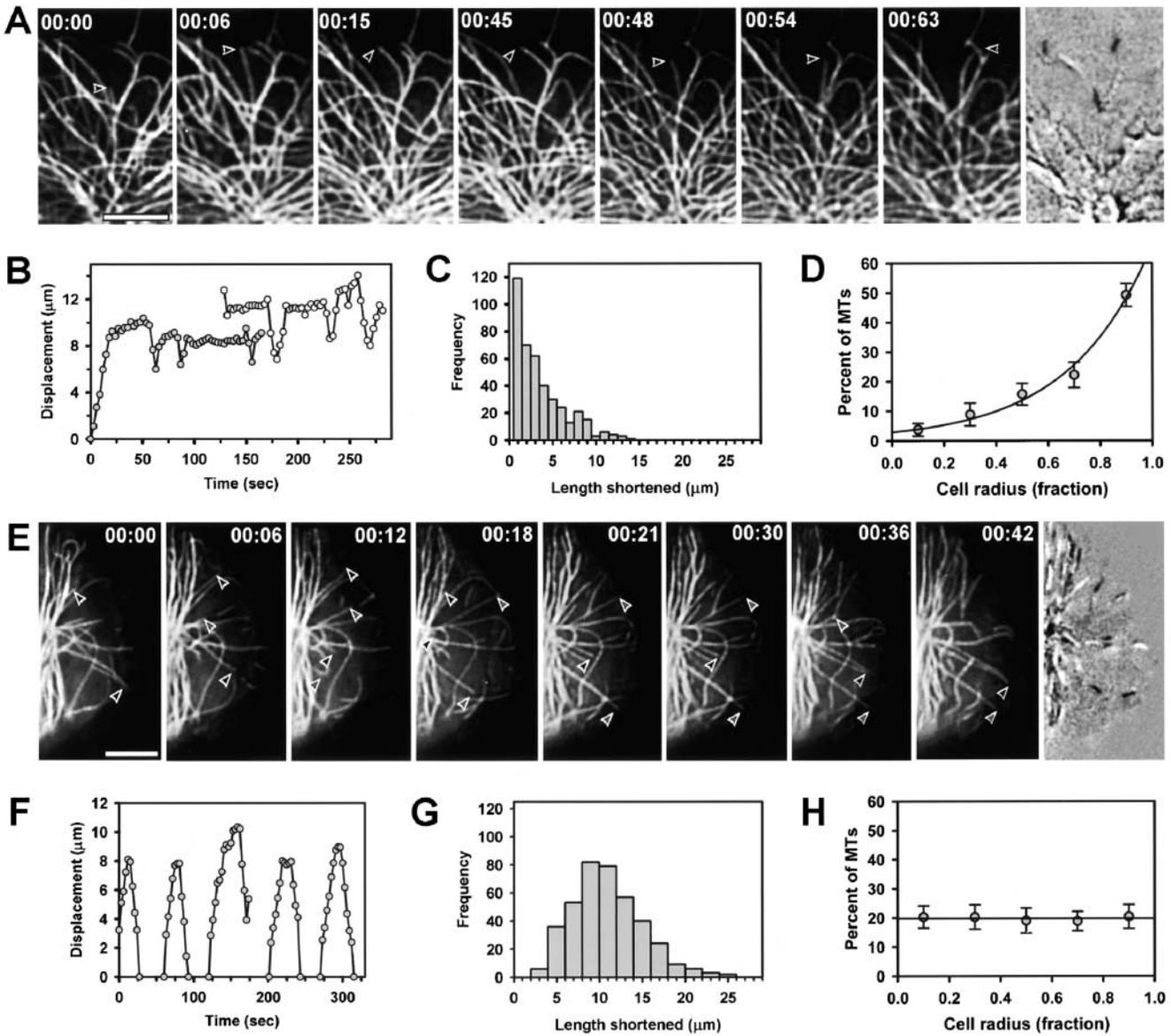
Figure 2. **Asymmetry of MT dynamics is determined by the presence of CLIPs at MT plus ends.** MTs show asymmetric behavior in control cells expressing EGFP (A, B, and C) and symmetric behavior in cells expressing EGFP–CLIP-170 Δhead mutant (D–F). (A) Time-lapse images of control cell show MT fluctuations at the cell margin. One MT is marked (arrowhead). The last image of the panel represents sequential subtraction analysis for identification of the active plus ends. Black and white segments represent MT growth and shortening, respectively, during the time interval. The active plus ends concentrate predominantly at the cell periphery. Numbers in the top right corners indicate time in s. Bar, 5 μm. (B) Life history plot of two MTs demonstrates asymmetric character of MT dynamics caused by persistent growth from centrosome and nonpersistent shortening from the cell margin. (C) The length distribution of shortening episodes is plotted in the histogram. Shortening of 400 MTs in eight cells (50 MTs per cell) were scored. MTs very rarely shortened back to the centrosome, and short episodes were frequent. (D) The distribution of the active plus ends along the cell radius is steeply ascending in control cells. Exponential curve fitting y = a·e^bx gives values of a = 2.8 ± 0.7 and b = 3.15 ± 0.3, which mean that the number of active plus ends is doubled every 5 μm if the cell radius is ~25 μm. 2,290 black and white segments were scored in four cells expressing GFP. (E) Absence of CLIPs at MT plus ends abolishes the fluctuating type behavior of MTs at the cell margin. Five MTs indicated by arrowheads demonstrate long phases of growth and shortening. Sequential subtraction analysis (last image of panel) demonstrates a uniform distribution of the active plus ends along the cell radius. Numbers in the top right corners indicate time in s. Bar, 5 μm. (F) Life histories of indicated MTs confirm their symmetric behavior where persistent growth from the centrosome to the cell margin is followed by persistent shortening from the cell margin back to the centrosome. The centrosome position is 0,0, and cell edge position is the point of transition from growth to shortening (catastrophes) on the life history plots. (G) Frequency histogram of the length shortened scored for 400 MT (n = 8 cells) demonstrates that long shortening was frequent. (H) Active plus ends are uniformly distributed in cells expressing GFP–CLIP-170 Δhead mutant. Exponential curve fitting gives values of a = 19.7 ± 0.8 and b = 0.00000 ± 0.07, which is equivalent to a straight line of essentially zero slope. The result means that the number of the active ends does not change along the cell radius. 1,787 black and white segments were scored in six cells expressing GFP–CLIP-170 Δhead mutant.

evaluate this possibility, we first confirmed the behavior of our EGFP–CLIP-170 head construct (aa 4–309). Direct imaging of living cells showed that the EGFP–CLIP-170 head

tracked MT plus ends (Fig. 4 A) similar to that of full-length CLIP-170. Also, MT dynamics were not detectably altered (unpublished data). The CLIP-170 head might be expected
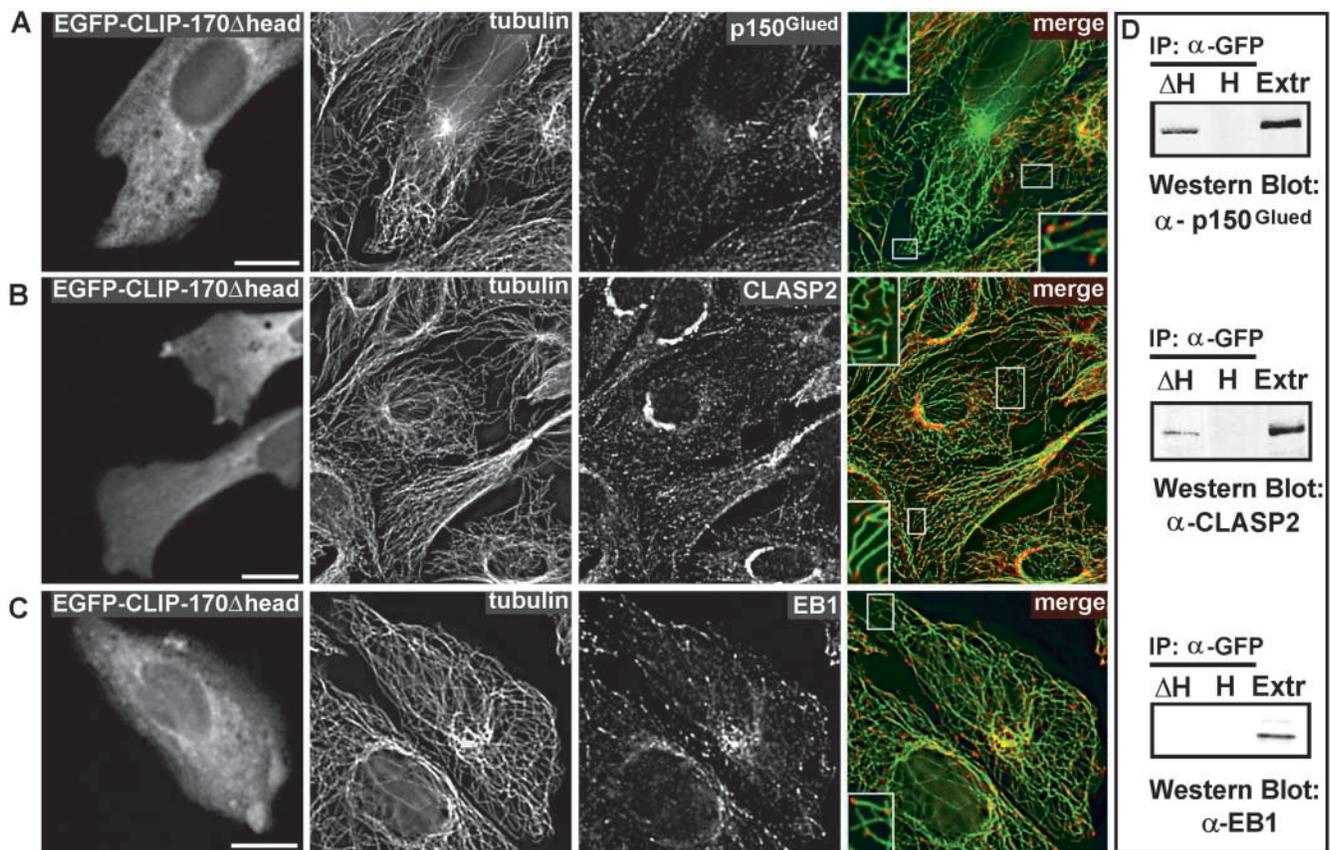
Figure 3. Distribution and interaction of p150^{Glued}, CLASP2, and EB1 in cells expressing GFP–CLIP-170 Δhead mutant. Cells were transiently transfected with GFP–CLIP-170 Δhead construct and processed for immunostaining with α-tubulin and α-p150^{Glued} (A), α-CLASP2 (B), or α-EB1 (C). (A) Presence of p150^{Glued} at MT plus ends seen in the control cells was completely abolished in the EGFP–CLIP-170 ΔH–positive cells. (B and C) Presence of CLASP2 and EB1 at the plus ends of MTs was not noticeably affected in the EGFP-positive cells. (Merged image) Green is tubulin, and red is p150^{Glued}, CLASP2, or EB1. The boxes show enlarged regions. Bar, 10 μm. (D) IP data show the interactions of p150^{Glued} and CLASP2 with EGFP–CLIP-170 Δhead mutant but not with the EGFP–CLIP-170 head mutant. No interaction was detected for EB1 with either CLIP construct.

to compete with endogenous CLIPs for binding sites on MT plus ends. However, expression of the EGFP–CLIP-170 head did not noticeably displace endogenous CLIP-170 (as evaluated by immunostaining with an antibody specific for CLIP-170) (Fig. 4 B). The result indicated that expression of the CLIP-170 head on the background of endogenous CLIPs was not adequate to test whether it was sufficient to support asymmetric MT dynamics.

Consequently, a rescue strategy was designed in which endogenous CLIPs were removed by overexpression of the CLIP-170 Δhead mutant, and rescue was attempted by simultaneous low level expression of the CLIP-170 head. The CLIP-170 Δhead mutant was fused to EBFP to visualize expression of the dominant negative mutant as distinct from that of the EGFP–CLIP-170 head. Expressed EBFP–CLIP-170 Δhead alone caused removal of endogenous CLIPs and alteration of MT dynamics in the same way as the EGFP–CLIP-170 Δhead construct (unpublished data). For the rescue experiment, we transfected cells by microinjecting into the nucleus a mixture of EBFP–CLIP-170 Δhead DNA and EGFP–CLIP-170 head DNA in a 10:1 molar ratio. Fig. 5 A shows a blue fluorescing cell, indicating overexpression of the CLIP-170 Δhead mutant and therefore removal of endogenous CLIPs from MT plus ends. In such cells, the EGFP–

CLIP-170 head localized to and tracked growing MT plus ends. Life history plots (Fig. 5 B) showed that asymmetric MT dynamics were restored. MTs underwent fluctuations near the cell margin and shortened only a small distance on average (3.6 ± 3.4 μm) before being rescued (Fig. 5, C and D), essentially the same as that in control cells. Analysis of MT dynamics showed that the CLIP-170 head restored the rescue frequency to control levels (Table I). This result establishes that the change in MT dynamics caused by removal of endogenous CLIPs through expression of the dominant negative mutant was mediated specifically by interaction of the CLIP head domain with the MT plus end.

Since expression of the CLIP-170 Δhead mutant caused p150^{Glued} to be removed along with endogenous CLIP-170, it was not clear whether the changes in MT dynamics resulting from removal of CLIP-170 were due to loss of the CLIP-170 head itself or to loss of p150^{Glued}. Similarly, restoration of dynamics due to rescue with the CLIP-170 head could be attributed, a priori, to either the CLIP head or recruitment of p150^{Glued}. To distinguish between these possibilities, we tested whether p150^{Glued} was recruited back to MT plus ends after expression of EGFP–CLIP-170 head in the rescue experiments. In contrast to the strong signal given by the expressed EGFP–CLIP-170 head, immunostaining failed to
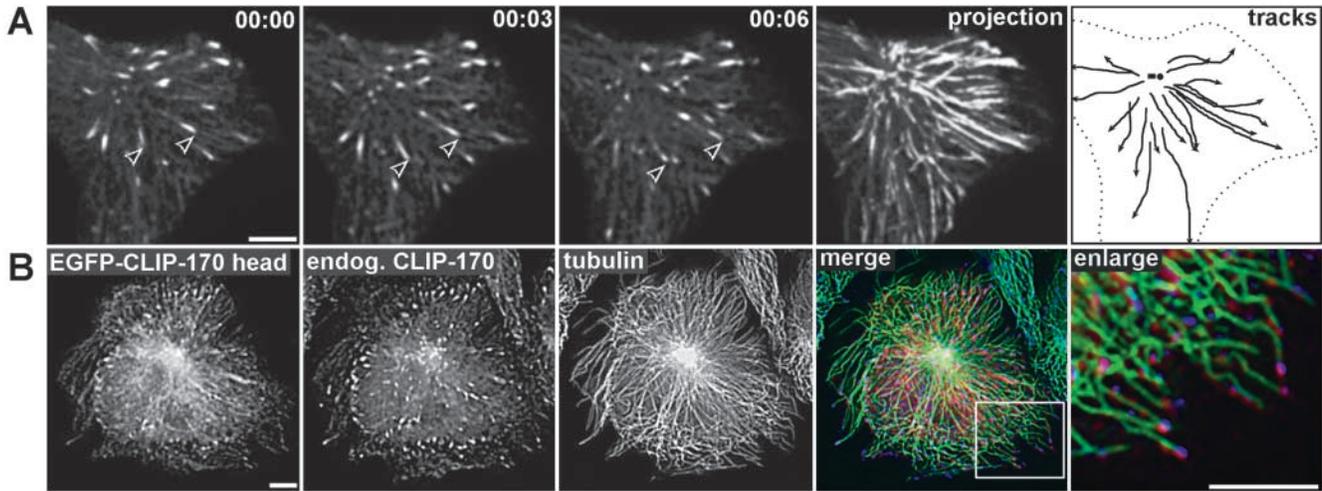
Figure 4. **CLIP-170 head tracks MT plus ends but does not displace endogenous CLIPs.** (A) Behavior of EGFP–CLIP-170 head. Time-lapse images show CLIP labels moving centrifugally from centrosome outward (arrowheads mark two comet tails). Time is in s. Long linear tracks of CLIP-170 head movements are demonstrated by projection analysis (generated by merging of successive frames within a stack) and are confirmed by trajectories of individual CLIP labels. Bar, 5 μm. (B) Endogenous CLIP-170 is not replaced by expressed EGFP–CLIP-170 head. CHO-K1 cells expressing a low level of EGFP–CLIP-170 head were processed for immunostaining using antibody against CLIP-170 (no. 2360; as described in Materials and methods) to visualize endogenous CLIP-170, anti-GFP to visualize the expressed EGFP–CLIP-170 head, and antitubulin to visualize MTs. The images show the same distribution for endogenous CLIP-170 and the GFP signal. (Merged image) Green is tubulin, red is EGFP-CLIP-170 head, and blue is endogenous CLIP-170. Colocalization at MT plus ends of endogenous CLIP-170 and expressed CLIP-170 head gives a magenta color. The boxed region is enlarged. Bar, 10 μm.

show significant accumulation of p150^{Glued} at MT plus ends (Fig. 5 E). Thus, p150^{Glued} was not recruited back along with the CLIP-170 head. This result indicates that restoration of normal MT dynamics did not require p150^{Glued}, suggesting that the CLIP-170 head domain was sufficient to function as a rescue factor.

The p150^{Glued} molecule contains the evolutionarily conserved CAP-Gly MT-binding sequence at its NH$_2$ terminus, similar to that in CLIPs (22 amino acids are identical over 43 residues) (Holzbaur et al., 1991). Although p150^{Glued} contains only one of two motifs present in the mammalian CLIP family, it nevertheless seemed possible that its head domain might provide function like the CLIP-170 head. Supporting this idea is the result that head of the p150^{Glued} is sufficient for MT plus end binding (Vaughan et al., 2002). Therefore, although p150^{Glued} was not necessary for normal MT dynamics, we tested whether it could support some level of normal dynamics in the absence of CLIPs. We used the same conditions as for the CLIP-170 head rescue experiment with one difference: we expressed an EGFP fusion of the first 311 amino acids of p150^{Glued}. As before, MT dynamics were analyzed by injecting Cy3 tubulin into cells expressing the EBFP–CLIP-170 Δhead and EGFP-p150^{Glued} head constructs. As before for CLIP-170, cells were selected for analysis in which the expressed p150^{Glued} head was specifically localized at the growing MT plus ends. By this criterion, we judged that expression levels of the CLIP-170 head and the p150^{Glued} head were approximately the same. Expression of the p150^{Glued} head domain increased the rescue frequency to 0.05 s^{-1} compared with 0.025 s^{-1} in cells expressing the CLIP-170 Δhead mutant and 0.17 s^{-1} in control cells or cells expressing the CLIP-170 head domain (Table I). Thus, unlike the CLIP-170 head domain the p150^{Glued} head was not sufficient to fully

restore MT dynamics. Nevertheless, the p150^{Glued} head did display some weak activity.

Discussion
CLIPs regulate MT dynamics by increasing rescue frequency

Normal MT dynamics in CHO-K1 and NRK cells (Komarova et al., 2002) and COS-7 cells (this study) are characterized by rapid growth, rapid shortening, and asymmetric transition frequencies, with the catastrophe frequency being low and the rescue frequency being high. A consequence of the combination of rapid growth and low catastrophe frequency is that MT growth is persistent. This means that nascent MTs frequently grow from the centrosome all the way to the cell margin without having undergone a transition to shortening phase. In contrast, a high rescue frequency means that MT shortening is nonpersistent. MTs typically shorten only a small distance back from the margin before their shortening is stopped and they resume growth. The result is a fluctuation type behavior in which MT plus ends tend to concentrate in the cell periphery and spend most of their lifetime there. Long MTs dominate over shorter ones, and MT turnover depends strongly on distance from the centrosome with turnover being rapid at the periphery and slow near the centrosome. The dynamic instability of MTs is thought to provide a mechanism by which MTs explore cytoplasmic space through alternating periods of growth and shortening (Kirschner and Mitchison, 1986). The property of asymmetric transition frequencies has the consequence that most of the exploration will take place in the vicinity of the cell margin.

Removal of CLIPs from MT plus ends decreased the rescue frequency, resulting in long shortening excursions.
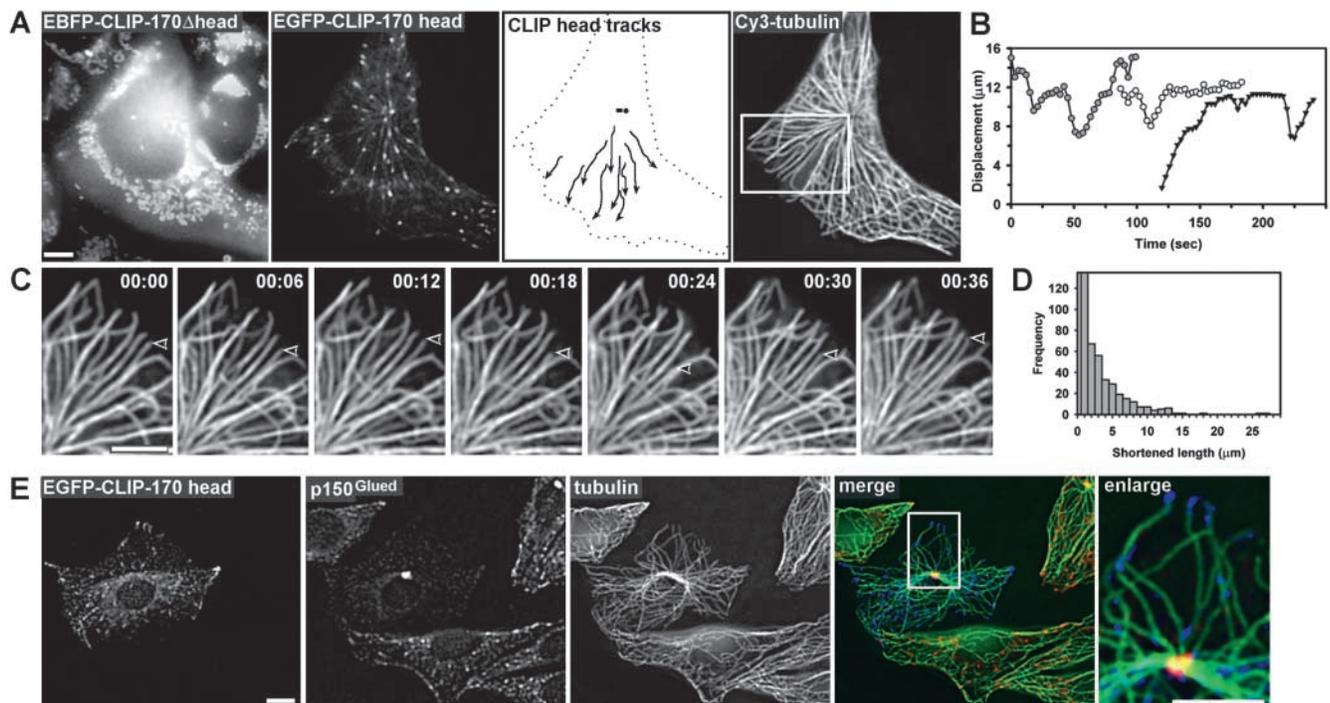
Figure 5. **CLIP-170 head is sufficient to restore MT dynamics.** (A) Cells were cotransfected with EBFP–CLIP-170 Δhead to remove endogenous CLIPs and EGFP–CLIP-170 head to test whether the CLIP-170 head could rescue MT dynamics. Blue fluorescence identifies cells expressing the EBFP–CLIP-170 Δhead mutant (small irregular dots near the nucleus are autofluorescence of mitochondria, which can also be seen in nontransfected cells). MT plus end localization of the CLIP-170 head was detected using an EGFP filter set. Individual CLIP-170 head labeling shows long tracks characteristic of normal MT dynamics. Cy-3–tubulin channel shows the MT pattern. Bar, 5 μm. (B) Life history plot demonstrates restoration of asymmetric MT behavior. Nascent MTs showed persistent growth with characteristic fluctuations near the cell margin. The centrosome position is 0,0. (C) Time-lapse images of MTs within enlarged region of A illustrates fluctuation near cell periphery (one MT is indicated by the arrowhead). Time shown in the top right corner is in s. Bar, 5 μm. (D) Frequency histogram of the shortening length. Pattern was characteristic of normal MT dynamics, namely, long shortening excursions were rare. (E) P150[Glued] is not recruited back to MT tips in the rescue experiment. CHO-K1 cells expressing both constructs, EBFP–CLIP-170 Δhead (not depicted) and EGFP–CLIP-170 head (depicted), were used for p150[Glued] immunostaining. P150[Glued] was not detected at MT tips in transfected cells, although it was present on MT plus ends in surrounding untransfected cells. (Merged image) Green is tubulin, red is p150[Glued], and blue is EGFP–CLIP-head. Bar, 10 μm.

Other parameters of MT dynamics did not change. Neither growth nor shortening velocities were affected, nor the catastrophe frequency. Consequently, MT growth remained persistent, and now MT shortening also became persistent. The result was an abrogation of asymmetric MT behavior. MT dynamics now consisted of repeated excursions of growth from the centrosome to the cell margin and shortening back to the centrosome. As a consequence, the distribution of MT plus ends through the cytoplasm became more uniform and turnover of MTs became more rapid even near their roots at the centrosome. The dynamic instability behavior of CLIP deficient MTs was to explore all of cytoplasmic space.

The normal function of CLIPs, by ensuring a high rescue frequency, may be to provide a mechanism by which MTs rapidly accommodate to the changing shape and advancing edge of motile cells. Concentration of the active plus ends of MTs at the cell periphery might also be an important feature of the MT cytoskeleton to achieve a fast response to changes in environmental conditions. For example, the Rho/mDia pathway selectively stabilizes a subset of MTs near the leading edge of migrating mammalian cells (Palazzo et al., 2001). Regional regulation of the MT turnover was also shown for HGF-treated PtK2 cells (Yvon and Wadsworth, 2000). CLIPs at growing MT plus ends interact with other

plus end–tracking proteins (Akhmanova et al., 2001; Coquelle et al., 2002; Tai et al., 2002) and might be involved in regulatory activities in addition to serving as a rescue factor. A recent report demonstrated that CLIPs interact with IQGAP1, possibly functioning as linkers between the plus ends of MTs and the cortical actin meshwork downstream of Rac1 and Cdc42 (Fukata et al., 2002). Thus, CLIPs are likely to be multifunctional proteins in which one domain modulates MT dynamics, whereas another domain serves a cross-talk function with the cell cortex.

The rescue activity of CLIPs localizes primarily to the head domain

Removal of endogenous CLIPs led to abnormally long MT-shortening excursions and also caused loss of p150[Glued] but not CLASP2 or EB1. Normal MT dynamics were restored by expression of the CLIP-170 head domain. However, p150[Glued] was not recruited back to MT plus ends. We conclude that the rescue activity of the CLIP-170 head domain does not require any part of CLIP's tail or associated proteins. However, it should be noted that this conclusion neither excludes the possibility that the head domain recruits a factor involved in rescue nor does it exclude important interactions for the CLIP tail domain in modulating the rescue activity of
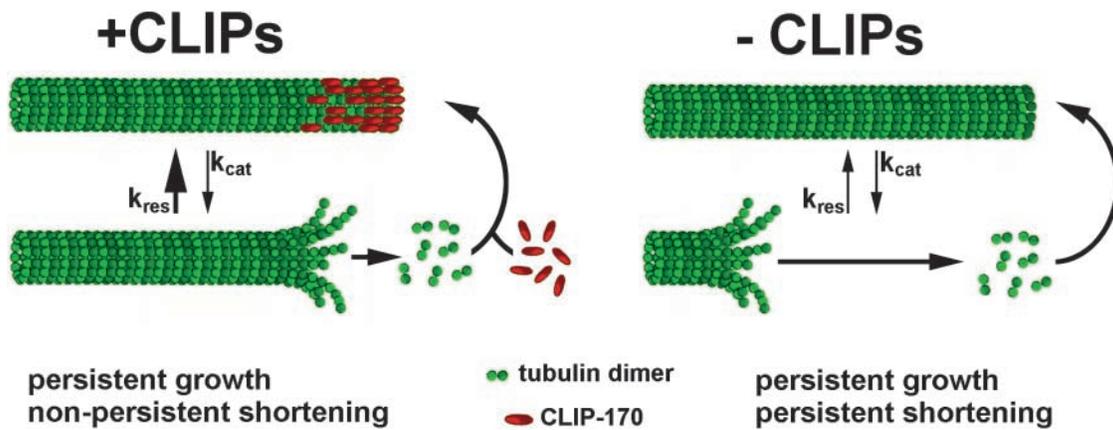
Figure 6. **Model for CLIP regulation of MT dynamics.** MTs with active CLIPs or head domain (+CLIP) show highly asymmetric MT behavior. Rescue frequency, k_{res} is ~50 fold higher than catastrophe frequency, k_{cat}, and MTs show persistent growth but nonpersistent shortening. When CLIPs are not available to bind MTs (−CLIP), the rescue frequency is greatly reduced. Now both MT growth and shortening are persistent. Thus, CLIPs play a role as rescue factors in MT dynamics.

the head, possibly by means of interaction with CLASP, p150^{Glued}, or Lis1 (Akhmanova et al., 2001; Coquelle et al., 2002; Tai et al., 2002). Since CLIP-115 contains essentially the same head domain as CLIP-170 (Hoogenraad et al., 2000), we infer that it too can function as a rescue factor. Thus, it seems that these two members of the CLIP family have redundant MT-related function. Consistent with this interpretation, enhanced recruitment of CLIP-170 to the plus ends of MTs was observed in primary fibroblasts isolated from CLIP-115 knockout mice, suggesting a compensatory role for CLIP-170 in regulation of MT dynamics under the condition of CLIP-115 deficiency (Hoogenraad et al., 2002). However, the lack of a metal-binding domain at the COOH terminus of CLIP-115 suggests that its tail domain may have interaction properties different from those of CLIP-170.

Unlike CLIP, p150^{Glued} did not increase the rescue frequency of MT dynamics to control levels, although it did restore MT dynamics to a limited extent. Since expression levels in vivo could not be controlled precisely, our comparative evaluation of p150^{Glued} and CLIP rescue activity must be regarded as preliminary. Although the results suggest that p150^{Glued} is not a primary regulator of MT dynamics, the partial restoration of MT behavior suggests that p150^{Glued} could function to enhance CLIP activity or partially substitute for it in the absence of CLIPs. Similar to CLIPs, the MT-related activity of p150^{Glued} is localized to its head domain and is not dependent on interaction with other dynactin components (Vaughan et al., 2002). The difference in the MT-related activities of CLIPs and p150^{Glued} may be related to the different number of CAP-Gly motifs in the head domain, CLIPs having two of them, whereas p150^{Glued} has only one. Together, the studies point to the importance of the CAP-Gly motif in regulation of MT dynamics.

Mechanism of CLIP displacement from MT plus ends by the Δhead mutant

Expression of the CLIP-170 Δhead mutant caused the removal of both CLIP species from MT plus ends with resultant changes in MT dynamics. These results indicate that the Δhead mutant acted in a dominant negative fashion. What

can be said about its mode of action? The simplest possibility, namely, competitive binding to the MT plus end is ruled out because the Δhead protein was not detected at MT plus ends. A second possibility is that the Δhead protein heterodimerized with endogenous CLIPs through its coiled-coil domain, thus making one headed dimers that were defective in binding to MT plus ends. This explanation is unlikely because CLIPs are known to homodimerize (Scheel et al., 1999; Hoogenraad et al., 2000). Homodimerization was substantiated by our coimmunoprecipitation experiments, which showed that EGFP-tagged full-length CLIP-170 did not pull down endogenous CLIP-170 or CLIP-115 and that neither EGFP nor HA-tagged Δhead protein pulled down CLIP-170. A third possibility for the mechanism of action of the Δhead protein is that it sequesters CLIPs by binding to them at a site critical for MT plus end interaction. Coimmunoprecipitation of the Δhead protein with CLIP-115 is consistent such an interpretation but failure to pull down CLIP-170 is not. A fourth possibility is that the Δhead protein titrates a factor necessary in the activation pathway for binding of CLIPs to MT plus ends. This explanation is consistent with all of the data, although it does not explain the difference in pull-down behavior of CLIP-170 and CLIP-115. The two CLIP paralogs differ in that CLIP-170 contains a COOH-terminal metal-binding motif that is absent in CLIP-115. Perhaps this difference is responsible for the difference in interaction with the Δhead protein. Clarification of the dominant negative mechanism will require a better understanding of the regulatory pathways governing CLIP association with MT plus ends. However, the fact that MT dynamics were completely restored by expression of the CLIP-170 head domain in the presence of the Δhead protein signifies that whatever binding partner might exist for the dominant negative, it is not essential for the MT binding or rescue activity of the CLIP head.

Model for CLIP regulation of MT dynamics

The principal result of this study is that CLIP-170 regulates MT dynamics either by serving as a rescue factor itself or by recruiting a factor that promotes MT rescue (Fig. 6). In this

respect, our conclusion differs from the proposal that the CLIP-170 ortholog, tip1p, in fission yeast functions as an anticatastrophe factor (Brunner and Nurse, 2000). Nevertheless, the two studies show substantial areas of agreement. In both studies, MT dynamics were modulated by removal of CLIPs or tip1p without changing the velocities of MT growth or shortening. In both studies, the biological function addressed was the mechanism by which MTs reach and explore the periphery of the cell. This biological result can be promoted either by decreasing the catastrophe frequency (anticatastrophe factor) or increasing the rescue frequency (rescue factor).

How might CLIPs function as rescue factors? CLIPs associate with growing plus ends, dissociate rapidly when MTs pause or shorten, and reassociate rapidly when MTs convert back to growth phase (Perez et al., 1999; Komarova et al., 2002). In addition, biochemical experiments showed that the CLIP-170 head domain interacts with nonpolymerized tubulin and promotes oligomerization (Diamantopoulos et al., 1999). The copolymerization of tubulin with CLIPs was proposed as a plausible mechanism for CLIP targeting specifically to growing plus ends (Diamantopoulos et al., 1999; Perez et al., 1999). Such targeting could be interpreted in terms of CLIPs serving either as anticatastrophe or rescue factors. Our results suggest a rescue factor model in which CLIPs bind tubulin dimers to form a CLIP–tubulin complex which then binds to a shortening MT and converts it to the growth phase.

Methods and methods

DNA constructs
All constructs used in the study are represented in Fig. 1 A. GFP constructs were generated in pEGFP-C1 vector (CLONTECH Laboratories, Inc.). The GFP–CLIP-170 construct contained rat brain CLIP-170 cDNA encoding aa 4–1,320 (Akhmanova et al., 2001); GFP–CLIP-170 head, aa 4–309; and GFP-CLIP-170 ΔH, aa 310–1,320. A separate GFP–CLIP-170 Δhead construct was made encoding aa 348–1,390 of human CLIP-170 cDNA (Pierre et al., 1992). The GFP-encoding part of this construct was substituted for by the BFP-encoding fragment of pEBFP-C1 to produce EBFP–CLIP-170 ΔH. The cDNA fragment encoding the NH$_2$-terminal 311 aa of the rat p150^{Glued} sequence was obtained by RT-PCR from rat brain RNA. It was verified by sequencing and subcloned into pEGFP-C1 expression vector to generate a GFP fusion. To generate HA-tagged fusions, the GFP-encoding part of the corresponding constructs was substituted for a sequence encoding a triple HA tag.

IPs
COS-1 cells were transfected by the DEAE-dextran method as described by Hoogenraad et al. (2000). CHO cells were transfected with Lipofectamine 2000 (Invitrogen Corporation) according to the protocol of the manufacturer. 24 or 48 h after transfection, cells were lysed in a buffer containing 20 mM Tris-HCl, pH 7.5, 100 mM NaCl, 0.5% NP-40, protease inhibitor cocktail (CH-4070; F. Hoffmann-La Roche Ltd.), phosphatase inhibitor cocktails 1 (1:200) and 2 (1:200) (Sigma-Aldrich). IPs were performed as described by Hoogenraad et al. (2000) using anti-GFP monoclonal antibodies (clones 7.1 and 13.1, CH-4070; F. Hoffmann-La Roche Ltd.) or anti-HA monoclonal antibody (clone 16B12; Covance Inc.). Western blots were prepared as described by Hoogenraad et al. (2000) using the following rabbit polyclonal antibodies: no. 2221, recognizing both CLIP-115 and CLIP-170 (Hoogenraad et al., 2000); no. 2360, specific for CLIP-170 (Coquelle et al., 2002); and no. 2358, recognizing CLASP2 (Akhmanova et al., 2001). mAbs against p150^{Glued} and EB1 were from BD Transduction Laboratories.

Immunostaining
CHO-K1 and COS-7 cells were transiently transfected by microinjection of DNA into the nucleus or by DEAE-dextran or Lipofectamine method (as described above). The constructs represented by Fig. 1 A were used for the

transfection. Cells were fixed as described elsewhere (Hoogenraad et al., 2000). Briefly, cells were fixed in cold methanol (−20°C) and postfixed by 3% formaldehyde. Incubation with 0.15% Triton X-100 was used for cell permeabilization after fixation. For immunostaining, we used the rabbit polyclonal antibodies: no. 2221 (used 1:200), recognizing both CLIP-115 and CLIP-170; no. 2360 (1:200), specific for CLIP-170 (Coquelle et al., 2002); and no. 2358 (1:200), recognizing CLASP2 (Akhmanova et al., 2001). Mouse monoclonal antibodies against p150^{Glued} and EB1 (1:100) were from BD Transduction Laboratories. Mouse monoclonal and rabbit polyclonal anti-GFP antibodies (1:100) (Molecular Probes) were used for triple immunostaining with other primary antibodies. Rat monoclonal antibody against α-tubulin (1:30) was a gift from J.V. Kilmartin (Laboratory of Molecular Biology, Cambridge, UK). Secondary antibodies were TRITC- and FITC-conjugated donkey anti–mouse and anti–rabbit and Cy5-coupled anti–rat (Jackson ImmunoResearch Laboratories). Stained cells were washed and mounted in Aqua-PolyMount medium (Polyscience, Inc.). Fixed samples were documented by fluorescence deconvolution microscopy using a Deltavision microscope system.

Quantification of proteins at MT plus ends
Quantification of the amount of plus end–tracking protein at MT tips was accomplished using double immunofluorescence staining for tubulin and one of the four following proteins: CLIPs, p150^{Glued}, EB1, and CLASP. The tip of an MT was defined as a square box, 5 pixels on a side (0.45 μm). Fluorescence intensities in each channel were measured with a CCD, background subtracted, and their ratio was computed. The ratio of signals plus end–tracking protein to tubulin in experimental cells was expressed as a percentage of the ratio in control cells which was taken as 100%. 80–130 MTs were analyzed in six to eight images for each control and experiment.

Cell culture, microinjection, and digital fluorescence imaging
CHO-K1 and NRK cells were grown in F-10 medium, COS-7, and BHK21 in DME-F12 medium supplemented with 10% FBS and antibiotics. For in vivo observation of MT dynamics, they were seeded onto coverslips with photoetched locator grids (Bellco Glass, Inc.). EGFP transfection was used as a control and EGFP–CLIP-170 Δhead or EBFP–CLIP-170 Δhead constructs were used for removal of endogenous CLIPs from MT plus ends. Cells were transiently transfected by glass capillary microinjection of DNA into the nucleus after the procedure of (Perez et al., 1999). EGFP, EGFP–CLIP-170 ΔH, and EBFP–CLIP-170Δhead were used at a needle concentration of 50 μg ml^{-1}. For rescue experiments, DNA of EBFP–CLIP-170 Δhead and EGFP–CLIP-170 head or with EGFP-p150^{Glued} head were mixed and comicroinjected. The final needle concentration of DNA for EBFP–CLIP-170Δhead vector was 100 μg ml^{-1}, whereas for EGFP–CLIP-170 head or EGFP-p150^{Glued} head vectors it was 10 μg ml^{-1}. The low needle concentration of EGFP–CLIP-170 head and EGFP-p150^{Glued} head gave sufficiently low expression levels of recombinant protein. Transfected cells were microinjected into the cytoplasm with Cy3-tagged tubulin at a needle concentration of 10 mg/ml. MT dynamics were observed 4–10 h after microinjection. Cells were kept on the microscope stage at 36–37°C during observation, and temperature was measured before and after each experiment. Cells were treated with the oxygen-depleting preparation, Oxyrase (Oxyrase, Inc.), during observation to reduce photodamage and photobleaching (Mikhailov and Gundersen, 1995). Injected cells were observed on a Nikon Diaphot 300 inverted microscope equipped with a Plan 100×, 1.25 NA objective using a Cy3 filter set for observations of Cy3-labeled MTs, a GFP filter set for observation of GFP fusion proteins, and a UV filter set for EBFP fusion protein. Images of 16-bit depth were collected with a CH350 slow scan, cooled CCD camera (Photometrics Ltd.) driven by Metamorph imaging software (Universal Imaging Corp.). The image was projected onto the CCD chip at a magnification of 250×, which corresponded to a resolution of 1 pixel = 0.09 μm (11.1 pixels per μm). Time-lapse series of 100–300 images were collected at 3-s intervals. 16-bit images were processed and rescaled with Metamorph software, and 8-bit images were prepared for presentation with Adobe Photoshop®.

Analysis of MT dynamics
The following parameters of MT dynamics were determined: instantaneous rates of growth and shortening, frequency of rescue and catastrophe transitions, and length of MT shortening from the cell edge. Data measurements were performed using 16-bit images in Metamorph software. SigmaPlot software (Jandel Scientific Corp.) was used for statistical analysis and plotting of graphs as described elsewhere (Komarova et al., 2002). Briefly, the lengths of individual MTs were measured from the centrosome (0,0 position of a centrosome), and life histories of MTs were plotted as length (μm) versus time (s). Instantaneous velocities were calculated as displacement of

the plus end between successive images (3 s) in a time-lapse series. The threshold of measurement was 2 pixels in the digital image, corresponding to 0.18 μm in the cell. Histograms of instantaneous velocities were generated for the MT population, and the mean values and SDs were computed. Cell margin was defined as a 3-μm zone from the cell boundary. The rate of the shortening was calculated from the histogram of instantaneous displacements of shortening MTs. For estimation of rescue and catastrophe frequencies, analyses of direct or subtracted images of MTs were used (Vorobjev et al., 1999). The transition probabilities were estimated as the ratio of number of transition events divided by the time of growth or shortening phase before a transition occurred. If an MT growing from the centrosome reached the cell edge without any transition to shortening, the time of the growth phase was included into overall data but not transition (catastrophe) was scored. The same method of estimation was used for determining rescue frequency of MTs shortening back from the cell margin (Komarova et al., 2002). The extent of MT shortening was expressed as the absolute distance shortened from the cell edge until the MT was rescued, and the data was presented as a frequency histogram.

Quantification of the MT length distribution along the cell radius was performed as described elsewhere (Komarova et al., 2002). Briefly, the cell radius was divided into five zones (each zone was a 0.2 fraction of the length of cell radius), and number of active ends, growing (black segments) and shortening (white segments) were scored for each zone. The result is represented as percent of the MTs within each zone where 100% is a total number of scored active plus ends of MTs in experiment or control. The data were fitted by least squares regression to a single exponential.

References

Akhmanova, A., C.C. Hoogenraad, K. Drabek, T. Stepanova, B. Dortland, T. Verkerk, W. Vermeulen, B.M. Burgering, C.I. De Zeeuw, F. Grosveld, and N. Galjart. 2001. Clasps are CLIP-115 and -170 associating proteins involved in the regional regulation of microtubule dynamics in motile fibroblasts. *Cell.* 104:923–935.

Brunner, D., and P. Nurse. 2000. CLIP170-like tip1p spatially organizes microtubular dynamics in fission yeast. *Cell.* 102:695–704.

Cassimeris, L., N.K. Pryer, and E.D. Salmon. 1988. Real-time observations of microtubule dynamic instability in living cells. *J. Cell Biol.* 107:2223–2231.

Coquelle, F.M., M. Caspi, F.P. Cordelieres, J.P. Dompierre, D.L. Dujardin, C. Koifman, P. Martin, C.C. Hoogenraad, A. Akhmanova, N. Galjart, et al. 2002. LIS1, CLIP-170's key to the dynein/dynactin pathway. *Mol. Cell. Biol.* 22:3089–3102.

Diamantopoulos, G.S., F. Perez, H.V. Goodson, G. Batelier, R. Melki, T.E. Kreis, and J.E. Rickard. 1999. Dynamic localization of CLIP-170 to microtubule plus ends is coupled to microtubule assembly. *J. Cell Biol.* 144:99–112.

Fukata, M., T. Watanabe, J. Noritake, M. Nakagawa, M. Yamaga, S. Kuroda, Y. Matsuura, A. Iwamatsu, F. Perez, and K. Kaibuchi. 2002. Rac1 and Cdc42 capture microtubules through IQGAP1 and CLIP-170. *Cell.* 109:873–885.

Heald, R. 2000. A dynamic duo of microtubule modulators. *Nat. Cell Biol.* 2:E11–E12.

Holzbaur, E.L., J.A. Hammarback, B.M. Paschal, N.G. Kravit, K.K. Pfister, and R.B. Vallee. 1991. Homology of a 150K cytoplasmic dynein-associated polypeptide with the *Drosophila* gene Glued. *Nature.* 351:579–583.

Hoogenraad, C.C., A. Akhmanova, F. Grosveld, C.I. De Zeeuw, and N. Galjart. 2000. Functional analysis of CLIP-115 and its binding to microtubules. *J. Cell Sci.* 113:2285–2297.

Hoogenraad, C.C., B. Koekkoek, A. Akhmanova, H. Krugers, B. Dortland, M. Miedema, A. van Alphen, W.M. Kistler, M. Jaegle, M. Koutsourakis, et al. 2002. Targeted mutation of Cyln2, in the Williams Syndrome critical region, links CLIP-115 haploinsufficiency to neurodevelopmental abnormalities. *Nat. Genet.* 32:116–127.

Hunter, A.W., and L. Wordeman. 2000. How motor proteins influence microtubule polymerization dynamics. *J. Cell Sci.* 113:4379–4389.

Kinoshita, K., I. Arnal, A. Desai, D.N. Drechsel, and A.A. Hyman. 2001. Reconstitution of physiological microtubule dynamics using purified components. *Science.* 294:1340–1343.

Kirschner, M.W., and T. Mitchison. 1986. Microtubule dynamics. *Nature.* 324:621.

Komarova, Y.A., I.A. Vorobjev, and G.G. Borisy. 2002. Life cycle of MTs: persistent growth in the cell interior, asymmetric transition frequencies and effects of the cell boundary. *J. Cell Sci.* 115:3527–3539.

Mikhailov, A.V., and G.G. Gundersen. 1995. Centripetal transport of microtubules in motile cells. *Cell Motil. Cytoskeleton.* 32:173–186.

Mimori-Kiyosue, Y., N. Shiina, and S. Tsukita. 2000a. Adenomatous polyposis coli (APC) protein moves along microtubules and concentrates at their growing ends in epithelial cells. *J. Cell Biol.* 148:505–518.

Mimori-Kiyosue, Y., N. Shiina, and S. Tsukita. 2000b. The dynamic behavior of the APC-binding protein EB1 on the distal ends of microtubules. *Curr. Biol.* 10:865–868.

Mitchison, T., and M. Kirschner. 1984. Dynamic instability of microtubule growth. *Nature.* 312:237–242.

Palazzo, A.F., T.A. Cook, A.S. Alberts, and G.G. Gundersen. 2001. mDia mediates Rho-regulated formation and orientation of stable microtubules. *Nat. Cell Biol.* 3:723–729.

Perez, F., G.S. Diamantopoulos, R. Stalder, and T.E. Kreis. 1999. CLIP-170 highlights growing microtubule ends in vivo. *Cell.* 96:517–527.

Pierre, P., J. Scheel, J.E. Rickard, and T.E. Kreis. 1992. CLIP-170 links endocytic vesicles to microtubules. *Cell.* 70:887–900.

Pierre, P., R. Pepperkok, and T.E. Kreis. 1994. Molecular characterization of two functional domains of CLIP-170 in vivo. *J. Cell Sci.* 107:1909–1920.

Rickard, J.E., and T.E. Kreis. 1990. Identification of a novel nucleotide-sensitive microtubule-binding protein in HeLa cells. *J. Cell Biol.* 110:1623–1633.

Sammak, P.J., G.J. Gorbsky, and G.G. Borisy. 1987. Microtubule dynamics in vivo: a test of mechanisms of turnover. *J. Cell Biol.* 104:395–405.

Scheel, J., P. Pierre, J.E. Rickard, G.S. Diamantopoulos, C. Valetti, F.G. van der Goot, M. Haner, U. Aebi, and T.E. Kreis. 1999. Purification and analysis of authentic CLIP-170 and recombinant fragments. *J. Biol. Chem.* 274:25883–25891.

Shelden, E., and P. Wadsworth. 1993. Observation and quantification of individual microtubule behavior in vivo: microtubule dynamics are cell-type specific. *J. Cell Biol.* 120:935–945.

Spittle, C., S. Charrasse, C. Larroque, and L. Cassimeris. 2000. The interaction of TOGp with microtubules and tubulin. *J. Biol. Chem.* 275:20748–20753.

Tai, C.Y., D.L. Dujardin, N.E. Faulkner, and R.B. Vallee. 2002. Role of dynein, dynactin, and CLIP-170 interactions in LIS1 kinetochore function. *J. Cell Biol.* 156:959–968.

Tournebize, R., A. Popov, K. Kinoshita, A.J. Ashford, S. Rybina, A. Pozniakovsky, T.U. Mayer, C.E. Walczak, E. Karsenti, and A.A. Hyman. 2000. Control of microtubule dynamics by the antagonistic activities of XMAP215 and XKCM1 in *Xenopus* egg extracts. *Nat. Cell Biol.* 2:13–19.

Valetti, C., D.M. Wetzel, M. Schrader, M.J. Hasbani, S.R. Gill, T.E. Kreis, and T.A. Schroer. 1999. Role of dynactin in endocytic traffic: effects of dynamitin overexpression and colocalization with CLIP-170. *Mol. Biol. Cell.* 10:4107–4120.

Vaughan, K.T., S.H. Tynan, N.E. Faulkner, C.J. Echeverri, and R.B. Vallee. 1999. Colocalization of cytoplasmic dynein with dynactin and CLIP-170 at microtubule distal ends. *J. Cell Sci.* 112:1437–1447.

Vaughan, P.S., P. Miura, M. Henderson, B. Byrne, and K.T. Vaughan. 2002. A role for regulated binding of p150[Glued] to microtubule plus ends in organelle transport. *J. Cell Biol.* 158:305–319.

Vorobjev, I.A., V.I. Rodionov, I.V. Maly, and G.G. Borisy. 1999. Contribution of plus and minus end pathways to microtubule turnover. *J. Cell Sci.* 112:2277–2289.

Vorobjev, I., V. Malikov, and V. Rodionov. 2001. Self-organization of a radial microtubule array by dynein-dependent nucleation of microtubules. *Proc. Natl. Acad. Sci. USA.* 98:10160–10165.

Waterman-Storer, C.M., and E.D. Salmon. 1997. Actomyosin-based retrograde flow of microtubules in the lamella of migrating epithelial cells influences microtubule dynamic instability and turnover and is associated with microtubule breakage and treadmilling. *J. Cell Biol.* 139:417–434.

Yvon, A.M., and P. Wadsworth. 1997. Non-centrosomal microtubule formation and measurement of minus end microtubule dynamics in A498 cells. *J. Cell Sci.* 110:2391–2401.

Yvon, A.M., and P. Wadsworth. 2000. Region-specific microtubule transport in motile cells. *J. Cell Biol.* 151:1003–1012.